

# Spin-orbit laser mode transfer via a classical analogue of quantum teleportation

B. Pinheiro da Silva, M. Astigarreta Leal, C. E. R. Souza, E. F. Galvão and A. Z. Khoury  
*Instituto de Física, Universidade Federal Fluminense, 24210-346 Niterói - RJ, Brasil*

(Dated: October 15, 2018)

We translate the quantum teleportation protocol into a sequence of coherent operations involving three degrees of freedom of a classical laser beam. The protocol, which we demonstrate experimentally, transfers the polarisation state of the input beam to the transverse mode of the output beam. The role of quantum entanglement is played by a non-separable mode describing the path and transverse degrees of freedom. Our protocol illustrates the possibility of new optical applications based on this intriguing classical analogue of quantum entanglement.

PACS numbers:

## I. INTRODUCTION

The tensor product structure of the vector space describing composite quantum systems is the key to the very definition of quantum entanglement. It was noticed many years ago [1] that the same mathematical structure arises in the description of classical optical fields, yielding what has been called classical entanglement or non-separability. This analogue of quantum entanglement allows us to translate quantum information concepts to the classical domain. Our first contribution to this topic was the demonstration of a topological phase acquired by maximally entangled qubits in the spin-orbit modes of a classical laser beam [2, 3]. Later, we investigated a Bell inequality to characterize the nonseparability between polarization and the spatial mode structure of classical paraxial beams [4]. This investigation was also later taken up in the single photon regime by other groups [5, 6]. Recently, the role of Bell inequalities in classical optics has drawn a fair amount of attention, being addressed in a series of papers [7–9]. This new understanding of classical non-separability resulted in new optical applications inspired by quantum information [10–17].

The possibility of using the polarization degree of freedom to control spatial modes has resulted in a number of applications both in classical and quantum optics. Examples include quantum image control [18], spin to orbital degree of freedom information transfer [19–21], quantum cryptography [22–24], controlled gates [25, 26], quantum games [27], environment-induced entanglement [28], quantum teleportation [29]. The coherent superposition of different transverse modes carrying orthogonal polarizations creates polarization vortices that have been proved useful for classical and quantum encoding of information [30–32].

One of the chief uses of quantum entanglement is information distribution based on quantum teleportation [33]. It enables one party (Alice), to transfer an arbitrary, unknown quantum state to a second party (Bob) via the use of previously shared quantum entanglement and classical communication [34–38]. An investigation of an optical analogue of the teleportation protocol has been recently reported in [39], in which states of orbital angular momentum were transferred to polarization.

Here we report on experiments in which we perform the interferometric transfer of arbitrary polarization modes to the transverse spatial structure of a paraxial, classical laser beam. This is achieved by mapping the steps of a single-qubit quantum teleportation protocol into a sequence of controlled optical mode operations. In our experiments, the role of quantum entanglement is played by a classical non-separable joint state of the path and transverse spatial degrees of freedom of the laser beam. Our protocol translates the relative ease of polarization preparation into the possibility of high-quality preparation of arbitrary states of transverse modes of a laser beam. Our results push further the analogy between classical and quantum entanglement, showing new optical applications are possible if we explore this analogy in depth.

Our paper is organized as follows. In section II we describe the optical modes we use to describe the different degrees-of-freedom we manipulate in our experiment. In section III we translate the steps of the quantum teleportation protocol to a series of operations on a classical laser beam. In section IV we describe the experimental setup and results, with some concluding remarks in section V.

## II. OPTICAL MODE STRUCTURE

Our experiment involves interference and polarization measurements on first-order paraxial beams. We will work in the computational basis of Laguerre-Gaussian modes of width  $w$ , carrying orbital angular momentum. Inside an interferometer, these modes are distributed between two alternative paths determined by the longitudinal propagation axes of the modes. For simplicity, we assume two axes lying parallel to the  $z$  direction of the coordinate system, lying a distance  $d \gg w$  apart from each other, so that the overlap between transverse modes belonging to different paths is negligible. We shall refer to these paths as 0 and 1 and designate their locations on the  $x - y$  plane by the coordinates  $(0, 0)$  and  $(d, 0)$ , respectively.

We describe the transverse modes in the normalized Laguerre-Gaussian basis and focus on the first order, two-

dimensional vector space. Their functional form is

$$\psi_{\pm}(\xi, \eta) = \frac{2}{\sqrt{\pi}} (\xi \pm i\eta) e^{-[(\xi^2 + \eta^2)(1 + i\bar{z}) - i\phi(\bar{z})]}, \quad (1)$$

where

$$\begin{aligned} \tilde{z} &= z/z_0, \\ (\xi, \eta) &= (x, y)/w(\tilde{z}), \\ w(\tilde{z}) &= w_0\sqrt{1 + \tilde{z}^2}, \\ \phi(\tilde{z}) &= \arctan(\tilde{z}), \end{aligned} \quad (2)$$

$z_0 = k w_0^2/2$  is the Rayleigh distance and  $w_0$  is the beam waist. The transverse coordinates  $(\xi, \eta)$  are relative to the path axes and normalized by the beam width. This arrangement is depicted in Fig.(1).

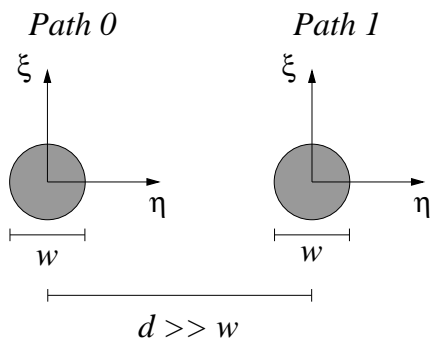


FIG. 1: Cross section view of the two-path propagation with the relative transverse coordinates.

Transverse modes lying on different paths do not overlap and are orthogonal, regardless of their functional form. Therefore, we can formally represent the path modes as an independent degree of freedom and describe them by a pair of column vectors

$$\chi_0 = \begin{bmatrix} 1 \\ 0 \end{bmatrix}, \quad \chi_1 = \begin{bmatrix} 0 \\ 1 \end{bmatrix}. \quad (3)$$

We then build the path-transverse mode structure as a tensor product  $\{\psi_+, \psi_-\} \otimes \{\chi_0, \chi_1\}$ . Finally, each transverse mode lying on each path has two possible polarizations described by horizontal and vertical unit vectors  $\{\hat{e}_H, \hat{e}_V\}$ . Thus, our complete workspace will be

$$\mathcal{W} = \{\psi_+, \psi_-\} \otimes \{\chi_0, \chi_1\} \otimes \{\hat{e}_H, \hat{e}_V\}. \quad (4)$$

These three degrees of freedom can be operated separately or in a combined way in order to implement controlled operations. In the polarization degree of freedom, unitary transformations are implemented with waveplates, and projections onto linear basis vectors are performed by polarizers. Transverse modes can be transformed by astigmatic mode converters or Dove prisms. Path modes can be operated on with beam splitters and phase shifters. Controlled operations are easily performed when transverse mode or polarization transformations are applied on one path only. With this set of

operations we will implement the steps of a quantum teleportation protocol to transfer an arbitrary polarization superposition to the transverse mode, using the resource of classical, non-separable states of the path and transverse degrees of freedom.

### III. THE PROTOCOL

The teleportation protocol involves three steps. First, an arbitrary polarization mode is prepared on the laser beam impinging on path 0. Then, the transverse mode is entangled with the path degree of freedom with a conditional operation. Finally, a Bell projection is performed on the path and polarization degrees of freedom, resulting in four transverse mode superpositions at the different outputs. One of them (the *successful* output) will carry a transversal mode state which directly corresponds to the initial polarisation state. The other three outputs will correspond to the initial polarisation state changed by Pauli operations, in direct correspondence with the one-qubit quantum teleportation protocol. In what follows we describe each step in more detail.

#### A. Polarization preparation

In order to demonstrate the protocol, we sent a sequence of twelve different polarization modes prepared with a half and a quarter waveplates. This sequence is represented in the Bloch sphere shown in Fig.(2), where the corresponding transverse modes produced are also represented. By rotating the orientations of the waveplates, we prepare polarisation states which interpolate between three mutually unbiased modes: *i*-) linear horizontal (point 1), *ii*-) linear at  $45^\circ$  (point 5) and *iii*-) left circular (point 9). Each point corresponds to a polarization superposition

$$\hat{\varphi}_n = \alpha_n \hat{e}_H + \beta_n \hat{e}_V \quad (1 \leq n \leq 12), \quad (5)$$

with  $\alpha_n$  and  $\beta_n$  determined by the polar and azimuthal angles on the sphere.

#### B. Path-transverse mode entanglement

A non-separable path-transverse mode state can be created by applying a path Hadamard operation followed by a conditional transverse mode flip. This is achieved with a Dove prism inserted on path 1 after the beam splitter, as sketched in Fig.(3).

#### C. Path-polarization Bell projection

An essential ingredient of the protocol is the ability to perform a Bell measurement in the degrees of freedom

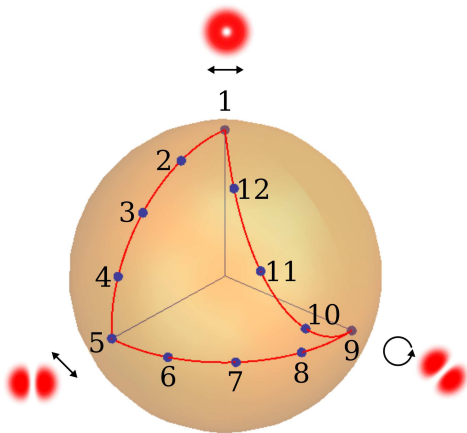


FIG. 2: Bloch sphere representation of the input polarization modes used in the teleportation protocol together with the corresponding output transverse modes.

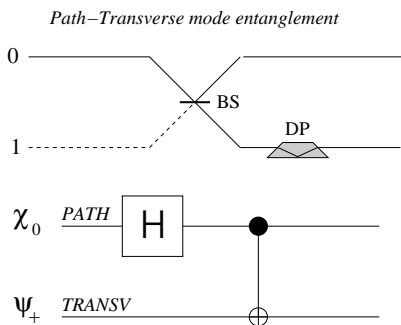


FIG. 3: Top: Path-transverse mode entanglement scheme. BS - beam splitter, DP - Dove prism. Bottom: Equivalent quantum circuit representation.

corresponding to the polarisation and beam path. This can be done via a controlled unitary gate between them, followed by a projection on single-system bases. In our scheme, we make a path dependent polarization transformation followed by a beam splitter operation (which corresponds to a Hadamard gate on the path mode), followed by polarization measurements with polarizing beam splitters. The path-polarization Bell measurement scheme is described at the top of Fig.(4). The controlled polarization transformation is implemented with a half waveplate oriented at  $45^\circ$ , placed on path 1. This corresponds to a CNOT gate that flips the polarization (target) conditioned to the path mode (control). Then, the two path modes are combined in a 50/50 beam splitter, corresponding to a Hadamard gate. One can easily verify that this sequence transforms the four path-polarization Bell modes as follows:

$$\begin{aligned}
 (\chi_0 \hat{e}_H + \chi_1 \hat{e}_V) / \sqrt{2} &\rightarrow \chi_0 \hat{e}_H, \\
 (\chi_0 \hat{e}_H - \chi_1 \hat{e}_V) / \sqrt{2} &\rightarrow \chi_1 \hat{e}_H, \\
 (\chi_0 \hat{e}_V + \chi_1 \hat{e}_H) / \sqrt{2} &\rightarrow \chi_0 \hat{e}_V, \\
 (\chi_0 \hat{e}_V - \chi_1 \hat{e}_H) / \sqrt{2} &\rightarrow \chi_1 \hat{e}_V.
 \end{aligned} \tag{6}$$

Finally, a polarization measurement performed at each output path can discriminate the four input Bell modes. These operations can be summarized as a quantum circuit, as shown at the bottom of Fig.(4).

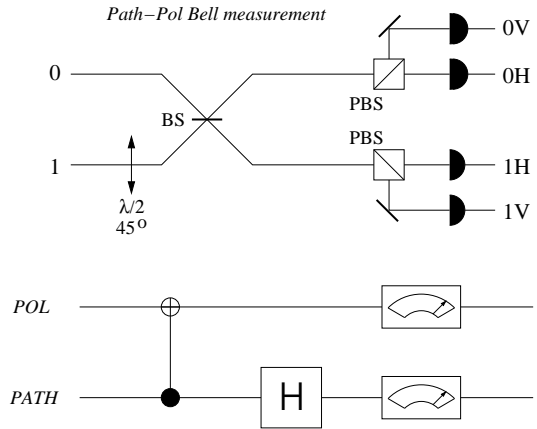


FIG. 4: Top: Path-polarization Bell projection scheme. Bottom: Equivalent quantum circuit representation.

#### IV. EXPERIMENTAL SETUP AND RESULTS

The experimental setup is described in Fig.(5). A horizontally polarized  $TEM_{00}$  mode produced by a He-Ne laser is diffracted by a holographic mask to prepare a Laguerre-Gaussian transverse mode  $\psi_+$  propagating on path  $\chi_0$ . Two waveplates convert its polarization to a chosen superposition

$$\hat{\phi} = \alpha \hat{e}_H + \beta \hat{e}_V, \tag{7}$$

thus preparing the initial separable supermode

$$\Psi_A = \psi_+(\eta, \xi) \chi_0 \hat{\phi}. \tag{8}$$

For simplicity, we shall omit the arguments in the transverse modes from now on. A beam splitter (BS) is used to perform a Hadamard gate in the path mode, and a Dove prism is inserted in output path 1 of the BS to flip the transverse mode propagating on this path. This operation is modelled by a CNOT gate on the transverse mode (target), controlled by the path; it creates the non-separable transverse-mode/path state which plays the role of a pair of maximally entangled qubits in the quantum teleportation protocol. This supermode is described by:

$$\Psi_B = \left[ \frac{\psi_+ \chi_0 + \psi_- \chi_1}{\sqrt{2}} \right] \hat{\phi}. \tag{9}$$

After the controlled operation between path and transverse mode, we start the sequence of operations that will perform the Bell projection on the path and polarization modes, as described in section II. First, a second controlled gate is performed by a half-wave plate oriented

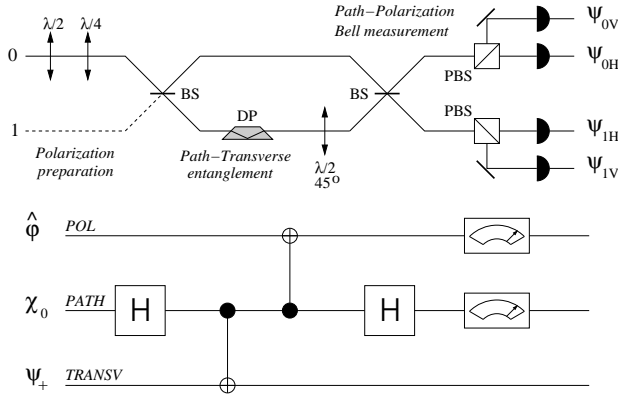


FIG. 5: Top: Experimental scheme for spin-orbit mode teleportation. Bottom: Equivalent quantum circuit representation.

at  $45^\circ$  (Pauli  $\sigma_X$  operation on polarization), inserted on path 1. It is equivalent to a CNOT gate on the polarization mode (target) controlled by the path, producing the supermode

$$\Psi_C = \frac{\psi_+ \chi_0 (\alpha \hat{e}_H + \beta \hat{e}_V) + \psi_- \chi_1 (\beta \hat{e}_H + \alpha \hat{e}_V)}{\sqrt{2}}. \quad (10)$$

Then, a Hadamard operation is performed on the path degree-of-freedom by a beam splitter, resulting in the output supermode

$$\begin{aligned} \Psi_D = & \left[ (\alpha \psi_+ + \beta \psi_-) \chi_0 \hat{e}_H \right. \\ & + (\beta \psi_+ + \alpha \psi_-) \chi_0 \hat{e}_V \\ & + (\alpha \psi_+ - \beta \psi_-) \chi_1 \hat{e}_H \\ & \left. + (\beta \psi_+ - \alpha \psi_-) \chi_1 \hat{e}_V \right] / 2. \end{aligned} \quad (11)$$

To complete the Bell measurement a polarization projection is performed with a polarizing beam splitter placed in each output path, giving output transverse modes

$$\psi_{ij}(\eta, \xi) = \left( \chi_i^\dagger \hat{e}_j^* \right) \cdot \Psi_D, \quad (12)$$

with  $i = 0, 1$  and  $j = H, V$ . The four output transverse modes are

$$\begin{aligned} \psi_{0H} &= \alpha \psi_+ + \beta \psi_-, \\ \psi_{0V} &= \beta \psi_+ + \alpha \psi_-, \\ \psi_{1H} &= \alpha \psi_+ - \beta \psi_-, \\ \psi_{1V} &= \beta \psi_+ - \alpha \psi_-. \end{aligned} \quad (13)$$

Output port  $0H$  is the successful one, which does not require any unitary correction, while ports  $0V$ ,  $1H$  and  $1V$ , must be corrected with  $\sigma_X$ ,  $\sigma_Z$  and  $\sigma_X \sigma_Z$  operations, respectively.

The four outputs were registered with a CCD camera. First we prepared the input beam with left circularly

polarized light, which corresponds to  $\alpha = 1/\sqrt{2}$  and  $\beta = i/\sqrt{2}$ . This setting is expected to produce four Hermite-Gaussian beams oriented at  $-45^\circ$  on port  $0H$ ,  $45^\circ$  on port  $0V$ ,  $45^\circ$  on port  $1H$  and  $-45^\circ$  on port  $1V$ , which is in very good agreement with the results shown in the top four images of Fig.(6). The bottom images are theoretical density plots of the transverse mode superpositions given by Eq.(13).

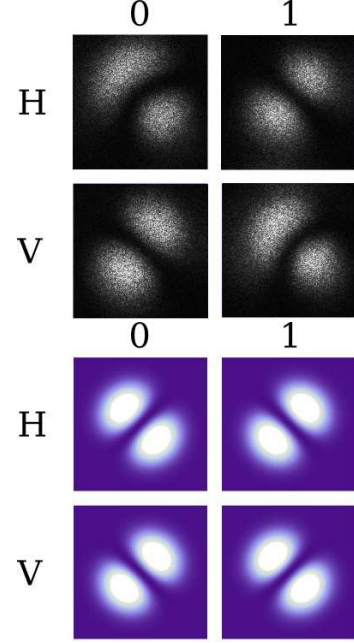


FIG. 6: Images of the four teleportation outputs for a circularly polarized input. Top: Experimental results. Bottom: Numerical simulations.

Then, a sequence of polarization modes was prepared by rotating the quarter and half waveplates at different orientations. This produced twelve polarization modes, forming a closed path in the Poincaré sphere, represented in Fig.(2). The images obtained in the successful port for these twelve input polarizations were registered on the CCD camera and shown in Fig.(7) together with the corresponding theoretical density plots of the expected transverse modes on this port. The experimental images are in good agreement with the numerical simulations.

## V. CONCLUSION

We have proposed and experimentally demonstrated a scheme to transfer an arbitrary polarization state to the first order transverse structure of a paraxial laser beam. The scheme mirrors the quantum teleportation protocol and uses operations on three internal degrees of freedom of a paraxial laser beam. It can be used as a practical way of generating arbitrary first order transverse modes either for classical optical processing or quantum cryptography in the photocount regime. A demonstration of

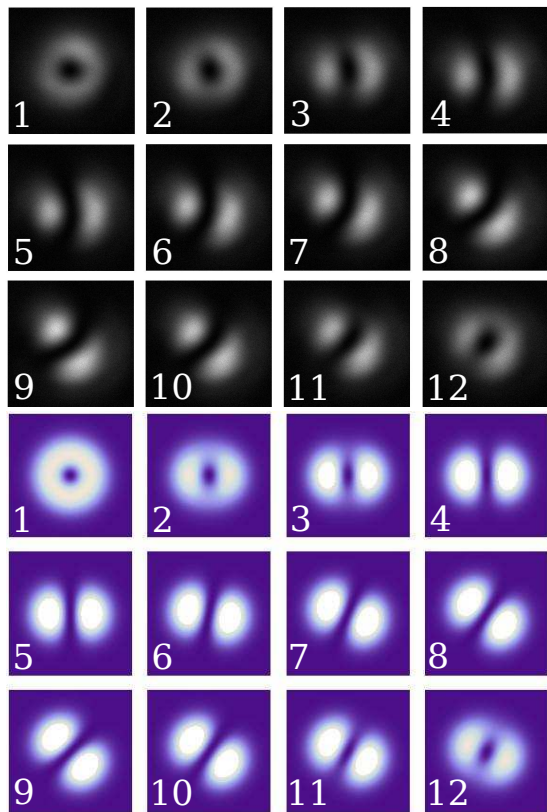


FIG. 7: Poincaré representation of the input polarization modes used in the teleportation protocol. Top: Experimental results. Bottom: Numerical simulations.

a protocol similar to the one implemented by us has been independently reported in Ref.[40].

### Acknowledgments

Funding was provided by Conselho Nacional de Desenvolvimento Tecnológico (CNPq), Coordenação de Aperfeiçoamento de Pessoal de Nível Superior (CAPES), Fundação de Amparo à Pesquisa do Estado do Rio de Janeiro (FAPERJ), and Instituto Nacional de Ciência e Tecnologia de Informação Quântica (INCT-CNPq).

- 
- [1] R. J. C. Spreeuw, “A classical analogy of entanglement,” *Found. Phys.* **28**, 361 (1998).
- [2] P. Milman, and R. Mosseri, “Topological Phase for Entangled Two-Qubit States,” *Phys. Rev. Lett.* **90**, 230403 (2003).
- [3] C. E. R. Souza, J. A. O. Huguenin, P. Milman, and A. Z. Khoury, “Topological phase for spin-orbit transformations on a laser beam,” *Phys. Rev. Lett.* **99**, 160401 (2007).
- [4] C. V. S. Borges, M. Hor-Meyll, J. A. O. Huguenin, and A. Z. Khoury, “Bell-like inequality for the spin-orbit separability of a laser beam,” *Phys. Rev. A* **82**, 033833 (2010).
- [5] L. Chen and W. She, “Single-photon spinorbit entanglement violating a Bell-like inequality,” *J. Opt. Soc. Am. B* **27**, A7 (2010).
- [6] E. Karimi, J. Leach, S. Slussarenko, B. Piccirillo, L. Marrucci, L. X. Chen, W. L. She, S. Franke-Arnold, M. J. Padgett, E. Santamato, “Spin-orbit hybrid entanglement of photons and quantum contextuality,” *Phys. Rev. A* **82**, 022115 (2010).
- [7] K. H. Kagalwala, G. Di Giuseppe, A. F. Abouraddy, and B. E.A. Saleh, “Bell’s measure in classical optical coherence,” *Nat. Photon.* **7**, 72 (2013).
- [8] X. F. Qian and J. H. Eberly, “Entanglement and classical polarization states,” *Opt. Lett.* **36**, 4110 (2011).
- [9] X. F. Qian, B. Little, J. C. Howell and J. H. Eberly, “Shifting the quantum-classical boundary: theory and experiment for statistically classical optical fields,” *Optica* **2**, 611 (2015).
- [10] B. N. Simon, S. Simon, F. Gori, M. Santarsiero, R. Borghi, N. Mukunda, and R. Simon, “Nonquantum entanglement resolves a basic issue in polarization optics,” *Phys. Rev. Lett.* **104**, 023901 (2010).
- [11] A. Holleczek, A. Aiello, C. Gabriel, C. Marquardt, and G. Leuchs, “Classical and quantum properties of cylindrically polarized states of light,” *Opt. Express.* **19**, 9714 (2011).
- [12] A. Aiello, F. Töppel, C. Marquardt, E. Giacobino, G. Leuchs, “Quantum-like nonseparable structures in optical beams,” *New J. Phys.* **17**, 043024 (2015).
- [13] P. Ghose and A. Mukherjee, “Entanglement in classical optics,” *Rev. Theor. Sci* **2**, 1 (2014).
- [14] F. Töppel, A. Aiello, C. Marquardt, E. Giacobino and G. Leuchs, “Classical entanglement in polarization metrology,” *New. J. Phys.* **16**, 073019 (2014).
- [15] M. McLaren, T. Konrad, and A. Forbes, “Measuring the nonseparability of vector vortex beams,” *Phys. Rev. A* **92**, 023833 (2015).
- [16] S. K. Goyal, F. S. Roux, A. Forbes, and T. Konrad, “Implementing quantum walks using orbital angular momentum of classical light,” *Phys. Rev. Lett.* **110**, 263602 (2013).
- [17] W. T. Buono, L. F. C. Moraes, J. A. O. Huguenin, C.

- E. R. Souza and A. Z. Khoury, "Arbitrary orbital angular momentum addition in second harmonic generation," *New Journal of Physics* **16**, 093041 (2014).
- [18] D. P. Caetano, P. H. Souto Ribeiro, J. T. C. Pardal, and A. Z. Khoury, "Quantum image control through polarization entanglement in parametric down-conversion," *Phys. Rev. A* **68**, 023805 (2003).
- [19] E. Nagali, F. Sciarrino, F. De Martini, L. Marrucci, B. Piccirillo, E. Karimi, and E. Santamato. "Quantum Information Transfer from Spin to Orbital Angular Momentum of Photons," *Phys. Rev. Lett.* **103**, 013601 (2009).
- [20] L. Chen and W. She, "Teleportation of a controllable orbital angular momentum generator," *Phys. Rev. A* **80**, 063831 (2009).
- [21] J. T. Barreiro, T.-C. Wei, and P. G. Kwiat, "Remote Preparation of Single-Photon Hybrid Entangled and Vector-Polarization States," *Phys. Rev. Lett.* **105**, 030407 (2010).
- [22] L. Aolita and S. P. Walborn. "Quantum Communication without Alignment using Multiple-Qubit Single-Photon States," *Phys. Rev. Lett.* **98**, 100501 (2007).
- [23] C. E. R. Souza, C. V. S. Borges, A. Z. Khoury, J. A. O. Huguenin, L. Aolita, and S. P. Walborn. "Quantum key distribution without a shared reference frame," *Phys. Rev. A* **77**, 032345 (2008).
- [24] V. D'Ambrosio, E. Nagali, S. P. Walborn, L. Aolita, S. Slussarenko, L. Marrucci, and F. Sciarrino "Complete experimental toolbox for alignment-free quantum communication," *Nat. Comm.* **3**, 961 (2012).
- [25] A. N. de Oliveira, S. P. Walborn, and C. H. Monken. "Implementing the Deutsch algorithm with polarization and transverse spatial modes," *J. Opt. B: Quantum Semiclass. Opt.* **7**, 288 (2005).
- [26] C. E. R. Souza and A. Z. Khoury, "A Michelson controlled-not gate with a single-lens astigmatic mode converter," *Opt. Express* **18**, 9207 (2010).
- [27] A. R. C. Pinheiro, C. E. R. Souza, D. P. Caetano, J. A. O. Huguenin, A. G. M. Schmidt and A. Z. Khoury, "Vector vortex implementation of a quantum game," *J. Opt. Soc. Am. B* **30**, 3210 (2013).
- [28] M. Hor-Meyll, A. Auyuanet, C. V. S. Borges, A. Aragão, J. A. O. Huguenin, A. Z. Khoury and L. Davidovich, "Environment-induced entanglement with a single photon," *Phys. Rev. A* **80**, 042327 (2009).
- [29] A. Z. Khoury and P. Milman, "Quantum teleportation in the spin-orbit variables of photon pairs," *Phys. Rev. A* **83**, 060301(R) (2011).
- [30] F. Cardano, E. Karimi, S. Slussarenko, L. Marrucci, C. de Lisio, and E. Santamato, "Polarization pattern of vector vortex beams generated by q-plates with different topological charges," *Appl. Opt.* **51**, C1-C6 (2012).
- [31] G. Milione, A. Dudley, T. A. Nguyen, K. Chakraborty, E. Karimi, A. Forbes, and R. R. Alfano, "Measuring the self-healing of the spatially inhomogeneous states of polarization of vector Bessel beams," *J. Opt.* **17**, 035617 (2015).
- [32] G. Milione, T. A. Nguyen, J. Leach, D. A. Nolan, and R. R. Alfano, "Using vector modes to encode information for optical communication," *Opt. Lett. (to appear)*.
- [33] C. H. Bennett, G. Brassard, C. Crepeau, R. Jozsa, A. Peres, and W. K. Wootters, "Teleporting an unknown quantum state via dual classical and Einstein-Podolsky-Rosen channels," *Phys. Rev. Lett.* **70**, 1895 (1993). <http://arxiv.org/abs/quant-ph/9708044>
- [34] D. Boschi, S. Branca, F. De Martini, L. Hardy, and S. Popescu, "Experimental Realization of Teleporting an Unknown Pure Quantum State via Dual Classical and Einstein-Podolsky-Rosen Channels," *Phys. Rev. Lett.* **80**, 1121 (1998).
- [35] D. Bouwmeester, J. Pan, K. Mattle, M. Eibl, H. Weinfurter, and A. Zeilinger, "Experimental quantum teleportation," *Nature (London)* **390**, 575 (1997).
- [36] S. Olmschenk, D. N. Matsukevich, P. Maunz, D. Hayes, L.-M. Duan, and C. Monroe, "Quantum Teleportation Between Distant Matter Qubits," *Science* **323**, 486 (2009)
- [37] L. Davidovich, N. Zagury, M. Brune, J.M. Raimond, and S. Haroche, "Teleportation of an atomic state between two cavities using nonlocal microwave fields," *Phys. Rev. A* **50**, 895 (1994).
- [38] S. Pirandola, J. Eisert, C. Weedbrook, A. Furusawa, S. L. Braunstein, "Advances in Quantum Teleportation", *Nature Photonics* **9**, 641-652 (2015).
- [39] S. M. H. Rafsanjani, M. Mirhosseini, O. S. Magaña-Loaiza, R. W. Boyd, "State transfer based on classical nonseparability," *Phys. Rev. A* **92**, 023827 (2015).
- [40] D. Guzman-Silva, R. Brüning, F. Zimmermann, C. Vetter, M. Gräfe, M. Heinrich, S. Nolte, M. Duparré, A. Aiello, M. Ornigotti, A. Szameit, "Demonstration of local teleportation using classical entanglement," <http://arxiv.org/abs/1509.06217> (2015).